

## Influence of the conversion coating on the corrosion of galvanized reinforcing steel

M.A. Arenas, C. Casado, V. Nobel-Pujol, J. de Damborenea \*

*Departamento de Corrosion y Proteccion, Centro Nacional de Investigaciones Metalúrgicas (CENIM/CSIC),  
Avenida de Gregorio del Amo 8, 28040 Madrid, Spain*

Available online 17 February 2006

### Abstract

Galvanized reinforcing steel with a cerium conversion coating have been studied in  $\text{Ca}(\text{OH})_2$  saturated solution with and without chlorides. Electrochemical results reveal that cerium conversion coating provides an effective corrosion resistance compared to galvanized steel at short immersion times, 5 days without  $\text{Cl}^-$  ions and 2 days with  $\text{Cl}^-$  in the solution. The results suggest that cerium layer inhibits hydrogen evolution on the galvanized coating at early stages. At longer immersion times, galvanized steel with cerium conversion coating and galvanized steel describe similar corrosion behaviour in both electrolytes. There is not significant differences in the corrosion current density, about  $5 \mu\text{A}/\text{cm}^2$ , due to the presence of chlorides ions in the  $\text{Ca}(\text{OH})_2$  saturated solution up to approximately 17 days of immersion. At longer immersion times, from 30 to 50 days, specimens in the chlorides containing solution exhibit higher corrosion activity than that recorded in the free  $\text{Cl}^-$  solution revealing that cerium layer cannot inhibit the localized attack promoted by chloride ions. © 2006 Elsevier Ltd. All rights reserved.

**Keywords:** Galvanized steel; Cerium conversion coating; Reinforcements; Inhibition

### 1. Introduction

Steel in concrete structures is normally protected from corrosion by a passive film due to the high alkalinity of the concrete. However, in presence of water and oxygen together with a sufficient amount of chlorides and/or carbon dioxide, this film can be destroyed and corrosion occurs. The corrosion products, whose volume is three times superior to that of iron, cause structure damages as cracks, accelerating the corrosion process. Among the existing protection methods to prevent steel corrosion in concrete, galvanized steel reinforcements are occasionally used to improve the corrosion resistance of important infrastructures in aggressive environment.

The protection of zinc is double: it acts as a physical barrier to aggressive agents and as a sacrificial anode because

of its less noble potential than steel one. The corrosion products of zinc present in the galvanized steel bars generate a protective barrier causing less concrete cover damage with respect to that determined by corrosion products produced with black steel bars. Moreover, as they are friable minerals, they can migrate to the adjacent concrete and fill voids and microcracks [1].

However, when zinc is immersed in wet cement, bubbles of hydrogen gas are formed. Hydrogen evolution on the rebar surface results from the attack of the zinc coating by the hydroxyl ions released into the concrete pore solution during cement hydration. Loss of adherence between galvanized reinforcements and concrete may result from this hydrogen evolution on the rebar surface occurring the first contact days. To prevent hydrogen evolution, zinc surfaces need to be passivated and chromate conversion coatings are commonly employed for zinc hot-dip coating. But chromates will be banned in 2007 because of its high toxicity. Cerium salts was chosen as environmentally friendly replacement based on previous paper results [2–5].

\* Corresponding author. Tel.: +34 915538900; fax: +34 915347425.  
E-mail address: [jdambo@cenim.csic.es](mailto:jdambo@cenim.csic.es) (J. de Damborenea).

The aim of this work is to develop cerium conversion coatings on galvanized reinforcements to study its stability and corrosion behaviour in an alkaline solution.  $\text{Ca}(\text{OH})_2$  saturated solution was used to simulate concrete at early stages and chloride ions were added to simulate degraded concrete. Moreover, it will be analysed if the passivation of the zinc surface by cerium layer is a valid preventive method of inhibiting hydrogen evolution.

## 2. Experimental

### 2.1. Materials

Corrugated reinforcements usually employed in construction, of 6 mm nominal diameter and 80 mm length, were used. Specimens were commercially hot dip galvanized by dipping in molten zinc (450 °C) for 1 min.

Cerium conversion coating was generated in a cerium containing solution by potentiostatic activation treatment during 10 min at constant temperature of 43 °C and pH of 1.3 [5]. The solution was prepared by addition in distilled water of cerium chloride  $\text{CeCl}_3 \cdot 7\text{H}_2\text{O}$  ( $10 \text{ g L}^{-1}$ ), 0.3 vol% of hydrogen peroxide  $\text{H}_2\text{O}_2$  and chlorhydric acid  $\text{HCl}$  (0.1 M) to adjust the pH at 1.3.  $\text{CeCl}_3$  rather than  $\text{Ce}(\text{NO}_3)_3$  has been used to form the coating since the more adherent and uniform coatings were obtained from chloride baths [6].

After treatment, the colour of the galvanized steel surface changes from shiny silver to shiny orange (just after) and yellowish (after 24 h) which visually confirms the growth of a cerium conversion coating (Fig. 1). Hereafter, galvanized steel will be named in the text as GS and galvanized steel with cerium conversion coating as CeGS.

### 2.2. Techniques

A conventional three-electrode cell was used: a saturated calomel electrode as reference electrode, a platinum wire as counter electrode and rebars as working electrode. The working area exposed is  $3 \text{ cm}^2$ , masking the rest of the rebar. Electrochemical tests were carried out with a potentiostat Gamry Instruments CMS 105 at room temperature ( $21 \pm 2$  °C).

$\text{Ca}(\text{OH})_2$  saturated solution was prepared with  $3 \text{ g L}^{-1}$  of  $\text{Ca}(\text{OH})_2$  in distilled water. The pH was 12.6. Chloride ions concentration in the solution is 0.5 M (3 wt.% NaCl). The pH of the chlorides containing solution was 12.55. After 30 days, the pH of the solution was about 9.60. Although carbonation has occurred, the galvanizing process provides effective protection against corrosion due to concrete carbonation [7]. According to Yeomans [8]

uncoated steel depassivates once the pH level drops below about 11.5, though in chloride-contaminated concrete this depassivation occurs at higher pH levels. In contrast, zinc coated steel in concrete remains passivated to pH levels of about 9.5 thereby offering substantial protection against the effects of carbonation of concrete. Hence, the carbonation should not be as critical as in the case of bare steel.

Open circuit potential,  $E_{\text{oc}}$ , was monitored with time during 30 days. Polarization resistance,  $R_p$ , was obtained from the slope of potentiodynamic scan carried out in the anodic direction from  $-10$  to  $+10$  mV vs  $E_{\text{oc}}$  at scan rate of  $1 \text{ mV/s}$ . Corrosion current density  $i_{\text{corr}}$  was estimated from polarization resistance  $R_p$  according to the Stern and Geary equation with a  $B$  constant value of  $26 \text{ mV}$ . Polarization curves  $I = f(E)$  were plotted with a scan rate of  $0.16 \text{ mV/s}$  from  $-50$  mV to  $+1100$  mV vs  $E_{\text{oc}}$  in the anodic direction followed by the reverse scan when a limit current density of  $0.025 \text{ A/cm}^2$  is reached.

GS and CeGS were investigated by scanning electron microscopy (SEM) coupled with energy dispersive spectrometer (EDS) (Oxford Instruments) and optical microscopy (Olympus PM3). Corrosion products of GS and CeGS samples immersed in  $\text{Ca}(\text{OH})_2$  saturated solution with 0.5 M of chlorides were analysed by X-ray diffraction (XRD) (Siemens D5000) using  $\text{CuK}\alpha$  radiation.

## 3. Results and discussion

### 3.1. Surface characterization of cerium conversion coating

Fig. 2 shows a cross section of CeGS with the typical morphology of hot-dipped galvanized steel as well as the

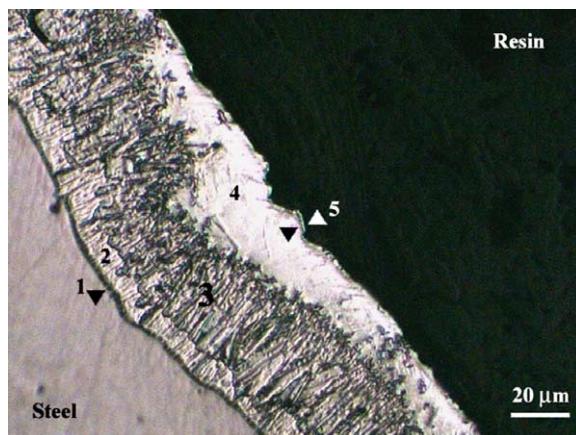


Fig. 2. Optical micrograph of galvanized steel with cerium conversion coating: (1) gamma ( $\Gamma$ ) phase, (2) delta ( $\delta$ ) phase, (3) zeta ( $\zeta$ ) phase, (4) eta ( $\eta$ ) phase, (5) cerium layer.



Fig. 1. Galvanized steel before (a) and 24 h after cerium treatment (b).

cerium conversion coating on the top of the upper layer. An observation by SEM of this cross section (Fig. 3(a)) confirms the presence of the cerium layer with a non-uniform thickness, from 0.8 up to 5  $\mu\text{m}$  depending on the area. Indeed, it can be observed a thicker layer of cerium around the corrugations due to the preferential deposition, (Fig. 3(b)).

In a previous work [5], it was pointed out that cerium conversion coating was mainly composed of a mixture of cerium ( $\text{Ce}^{3+}$  and  $\text{Ce}^{4+}$ ) hydrated oxides/hydroxides with zinc oxide  $\text{ZnO}$ . Nevertheless, chlorides are detected by EDS analysis probably forming stable compounds, as zinc hydroxide/oxides or cerium oxychloride. The presence of these chlorides is due to that  $\text{CeCl}_3$  is the precursor to form the layer. Chloride ions will not be free in the pore solution of the concrete and hence, will not behave as aggressive

agents to zinc coating. As it is well known, zinc hydroxy-chlorides is formed on the surface of galvanised steel in chloride contaminated concrete and causes cracking of concrete cover [9].

The presence of these zinc oxides is due to the conditions used to create the cerium layer: an acidic pH which is known to attack zinc and a strong oxidant such as  $\text{H}_2\text{O}_2$  [2].

### 3.2. Electrochemical results

To test the corrosion behaviour of the specimens at early immersion stages in alkaline medium,  $\text{Ca}(\text{OH})_2$  saturated solution, polarization curves were plotted after immersion for 15 min (Fig. 4). Both specimens reveal a passive region of about 1000 mV. CeGS exhibits lower passive current

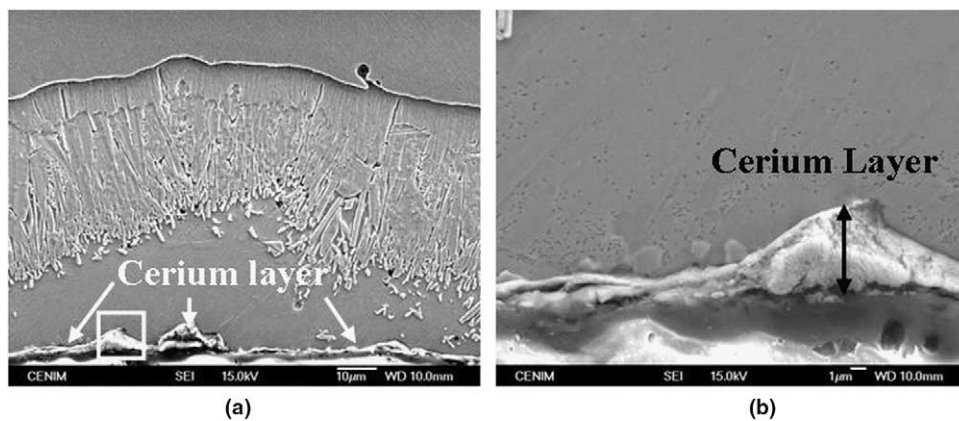


Fig. 3. SEM micrograph (a) of the galvanized steel with cerium conversion coating and (b) detail of cerium layer: thickness of 4.5  $\mu\text{m}$ .

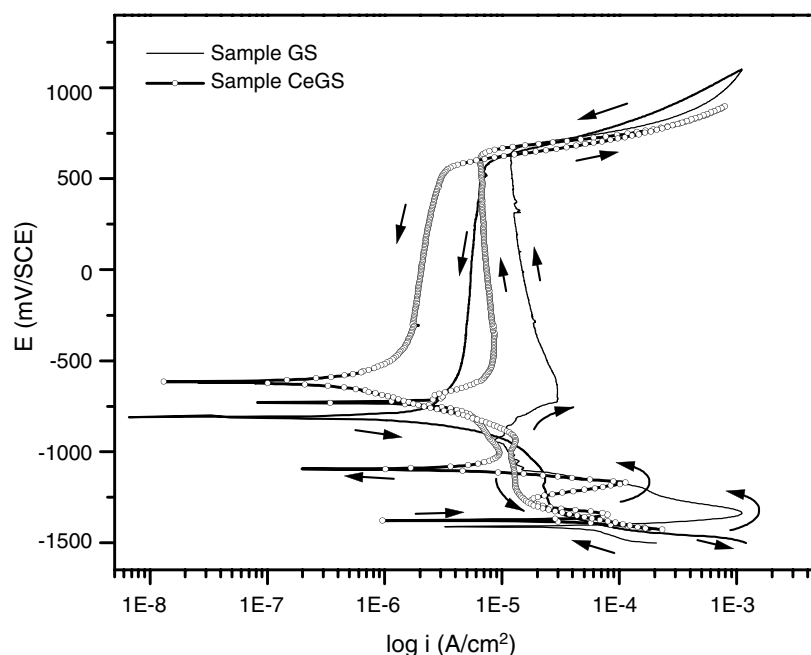


Fig. 4. Cyclic polarization curves for GS and CeGS in  $\text{Ca}(\text{OH})_2$  saturated solution.

density, about  $7 \mu\text{A}/\text{cm}^2$ , than GS, about  $19 \mu\text{A}/\text{cm}^2$ . At higher potential than 600 mV, the decomposition of the medium is described by means of current density increase.

Reverse scan for CeGS and GS shows lower current density values compared to that found in the direct sweep. This behaviour is due to the protective characteristics of the oxide layer generated during the anodic polarization. CeGS describes lower current density than GS which can be related to the different nature of the passive layer as cerium is presented on the surface. It can be concluded that CeGS in  $\text{Ca}(\text{OH})_2$  saturated solution presents higher stability than GS at early immersion stages. Therefore, cerium conversion layer offers an extra corrosion resistance to GS at short immersion time.

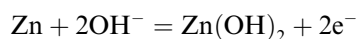
At longer exposure times, electrochemical behaviour of GS and CeGS was characterised by the evolution of the open circuit potential,  $E_{\text{oc}}$ , and corrosion current density,  $i_{\text{corr}}$ , with time in  $\text{Ca}(\text{OH})_2$  saturated solution (Fig. 5). It can be seen that GS and CeGS behave differently up to 9 days. Until 4 days in solution, open circuit potential values for GS increase slightly from  $-1370$  to  $-1330$  mV/SCE and corro-

sion current density values vary from  $70$  to  $35 \mu\text{A}/\text{cm}^2$ . The open circuit potential values are in agreement with those reported in literature for galvanized steel in this medium [9]. Similarly for CeGS, a relative stability for open circuit potential and corrosion current density is also observed.  $E_{\text{oc}}$  varies from  $-577$  to  $-685$  mV/SCE, and  $i_{\text{corr}}$  decreases from  $3$  to  $1.5 \mu\text{A}/\text{cm}^2$ . Then, CeGS provides better corrosion protection at early exposure stages since higher  $E_{\text{oc}}$  and lower  $i_{\text{corr}}$  values than those for GS are recorded.

Changes occur for both specimens following 5–9 immersion days. For GS,  $E_{\text{oc}}$  shifts to nobler values, from  $-1330$  mV/SCE to  $-620$  mV/SCE, whereas  $i_{\text{corr}}$  value decreases from  $35$  to  $1 \mu\text{A}/\text{cm}^2$ . This behaviour is related to the zinc passivation process of the galvanized steel immersed in an alkaline environment which is normally observed with the potential transition from the active state ( $E_{\text{oc}}$  around  $-1300$  or  $-1400$  vs SCE) to passive state ( $E_{\text{oc}}$  around  $-650$  or  $-700$  vs SCE). Conversely, for CeGS, open circuit potential and corrosion current density remain relatively stable,  $-685$  mV/SCE and  $1.5 \mu\text{A}/\text{cm}^2$ , respectively. Hence,  $E_{\text{oc}}$  and  $i_{\text{corr}}$  are similar for both materials at 9 days of immersion.

Visual observations done during the initial stages, up to 9 days, confirm the different corrosion behaviour for GS and CeGS. It was observed hydrogen release as bubbles of gas on the surface of GS but not on CeGS. Moreover, a white, opaque and uniform film is formed on the surface of GS while a non-uniform layer is formed for CeGS.

Anodic dissolution of Zinc in  $\text{Ca}(\text{OH})_2$  involves a complex series of reactions including the following steps. Zinc dissolves in the alkaline to give a complex hydroxyzincate [10]:



In saturated calcium hydroxide solution the earlier reactions given are followed by the precipitation of a layer of calcium hydroxyzincate,  $\text{Ca}[\text{Zn}(\text{OH})_3]_2\text{H}_2\text{O}$ .

The anodic dissolution of zinc could be inhibited by cerium presence on the surface avoiding the calcium hydroxyzincate formation on the whole surface. Hence, the formation of the passive layer could be only expected on the defective areas of the cerium conversion coating.

The results suggest that cerium conversion coating provides an effective corrosion resistance up to 5 days of immersion. The cerium layer seems to inhibit the initial hydrogen evolution that occurs on the galvanized surface during the early exposure times showing  $i_{\text{corr}}$  values about two orders of magnitude lower than that recorded for GS. However, as immersion time increases, the passive layer is formed on the GS surface and the  $i_{\text{corr}}$  values are similar to that obtained for cerium layer. Thus, the effectiveness of the cerium coating would refer to the initial stages when an extra protection is needed.

On the other hand, it should be mentioned that the corrosion of CeGS in saturated  $\text{Ca}(\text{OH})_2$  and in concrete may

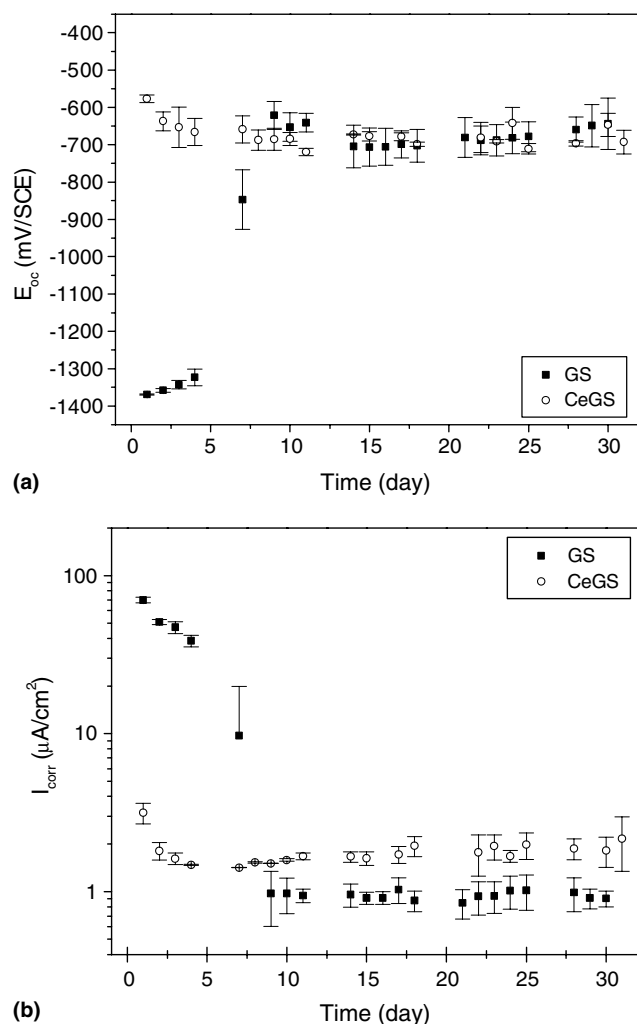


Fig. 5. Variation of the open circuit potential (a) and current density (b) values with time for GS and CeGS in  $\text{Ca}(\text{OH})_2$  saturated solution.



not be the same due to that the experimental conditions could accelerate the corrosion process and higher effective protection could be expected for embedded CeGS rebars. However, it must keep in mind that once the cerium ions have precipitated on the surface, they will be immobilized in the concrete not waiting further inhibitory properties. Cement has the potential to be very effective immobilisation matrix for actinide (III, IV) elements. Indeed, C–H–S is demonstrated to have an insolubilising effect on cerium, leading to precipitation and compound formation [11].

At longer immersion times, from 10 to 30 days, open circuit potential and current density values of both specimens remain similar and “relatively stable”, about  $-700$  mV for  $E_{oc}$  and  $1 \mu\text{A}/\text{cm}^2$  for  $i_{corr}$ . The results confirm that at longer immersion time the presence of the cerium conversion coating does not hinder the formation of the passive layer on GS due to the alkaline conditions.

In presence of chlorides, polarization curves after 15 min of immersion reveal a passive behaviour for both specimens. GS exhibits a passive region of about 300 mV and a passive current density of about  $15 \mu\text{A}/\text{cm}^2$  whereas CeGS shows an anodic branch which current density decreases with the anodic potential sweep reaching similar current densities than GS at  $-850$  mV (Fig. 6). Peaks observed in the direct anodic sweep of GS are related to the formation of pseudo-passive intermediate states before reaching the passive state.

On the other hand, CeGS provides better resistance to localized attack because of breakdown of passivity occurs at  $-742$  mV/SCE against  $-850$  mV/SCE for GS as it can be observed in the curve by means of anodic current density increase. After attaining pitting potential, during the anodic reverse scan the curve intersects the intensity axis at a potential at which neither anodic oxidation nor cathodic reduction can occur, i.e., pitting is arrested. This potential is referred to as the protection potential  $E_p$  against pitting, since at and below  $E_p$  the metal, will not pit and

the whole surface will remain passive. Pitting will occur only in the range of potentials between  $E_p$  and pitting potential if the surface is already pitted. Hence, between  $E_p$  and pitting potential prior pits will continue to propagate, but initiation of new ones will not be possible [12].

In conclusion, at early immersion stages in  $\text{Ca}(\text{OH})_2$  saturated solution containing  $0.5 \text{ M}$  of  $\text{Cl}^-$ , GS and CeGS describe similar corrosion current densities but CeGS decreases the pitting susceptibility by increasing the pitting potential in about 100 mV compared to GS.

Fig. 7 presents the evolution of the open circuit potential,  $E_{oc}$ , and corrosion current density,  $i_{corr}$ , with time in  $\text{Ca}(\text{OH})_2$  saturated solution containing  $0.5 \text{ M}$   $\text{Cl}^-$ .

During one day of immersion, CeGS and GS behave differently. Indeed, GS reveals a  $E_{oc}$  value of about  $-1370$  mV/SCE, and  $i_{corr}$  about  $130 \mu\text{A}/\text{cm}^2$ , whereas CeGS exhibits a value of  $-767$  mV/SCE for  $E_{oc}$  and  $3 \mu\text{A}/\text{cm}^2$  for  $i_{corr}$ . CeGS improves the corrosion behaviour to GS for this exposure time.

The second day of immersion, values of open circuit potential and corrosion current density for CeGS have

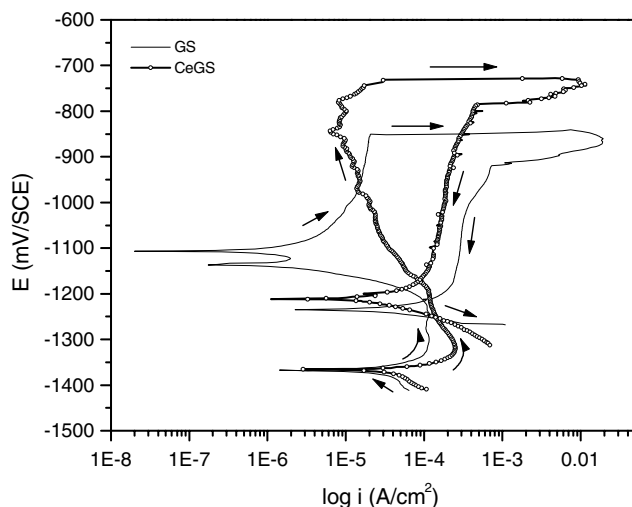


Fig. 6. Cyclic polarization curves for GS and CeGS in  $\text{Ca}(\text{OH})_2$  saturated solution  $+0.5 \text{ M}$   $\text{Cl}^-$ .

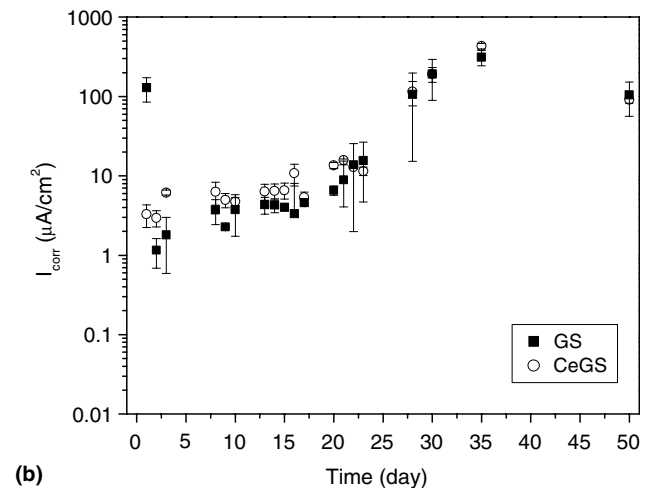
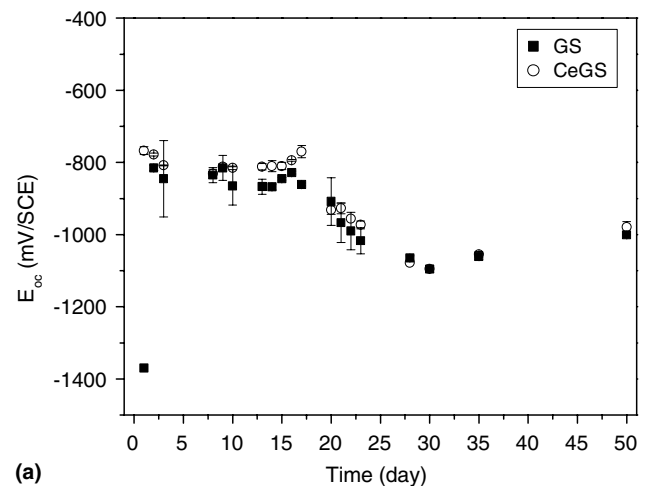


Fig. 7. Variation of the open circuit potential (a) and current density values (b) with time for GS and CeGS in  $\text{Ca}(\text{OH})_2$  saturated solution  $+0.5 \text{ M}$   $\text{Cl}^-$ .

not changed. However, open circuit potential increases to  $-815$  mV/SCE and a corrosion current density decreases to  $1 \mu\text{A}/\text{cm}^2$  for GS. The  $i_{\text{corr}}$  decrease is related to the formation of the passive layer on the galvanized steel surface in the alkaline solution.

Until 17 days, CeGS reveals a slow shift to nobler potential, around  $-760$  mV/SCE, while the  $E_{\text{oc}}$  value of GS decreases to  $-860$  mV/SCE. Similar current density values have been found for both specimens, about  $5 \mu\text{A}/\text{cm}^2$ . CeGS and GS exhibit non-significant changes in the  $i_{\text{corr}}$  compared to the initial values. Moreover,  $i_{\text{corr}}$  values are about the same order of magnitude than those measured in the absence of chlorides. However, as immersion time increases, from 17 to 30 days, both specimens exhibit a more severe corrosion process compared to that observed in the free chlorides solution. This is, current density values of about  $110 \mu\text{A}/\text{cm}^2$  and  $E_{\text{oc}}$  values of about  $-1065$  mV/SCE after approximately 28 days. The  $i_{\text{corr}}$  increase indicates that the protective layer does not confer to galvanized steel a good chlorides resistance at these exposure times.

Visual observations after 30 days immersion, reveals hydrogen bubbles on CeGS surface which indicates that zinc surface has become accessible to chlorides. Therefore, cerium layer does not offer an extra protection against the aggressive agents and any passivation is produced. Surface is corroded and a large area of zinc is exposed to the medium.

Immersion time was then extended to 50 days in order to study GeCS and GS behaviour in presence of chlorides. From 31 to 50 immersion days,  $E_{\text{oc}}$  shift to more positive values about  $-980$  mV/SCE for CeGS and  $-1001$  mV/SCE for GS. Current density values increase to about  $430 \mu\text{A}/\text{cm}^2$  for CeGS and  $312 \mu\text{A}/\text{cm}^2$  for GS following 35 exposure days and finally, strongly decrease to  $100 \mu\text{A}/\text{cm}^2$ .

Fig. 8 shows the surface appearance of specimens after 30 days of immersion in saturated  $\text{Ca}(\text{OH})_2$  solution. As can be observed, clear evidence of attack is revealed compared to the initial surface (Fig. 1). GS surface is covered by a white layer and CeGS also reveals small white grains on the surface. After immersion in a chloride containing solution, similar changes are shown. In this case, the amount of the corrosion products increases for both specimens and white grains are also observed for GS. Moreover, the colour surface of CeGS has turned to grayish but cerium conversion coating remains visually observable in some place especially around the corrugations.

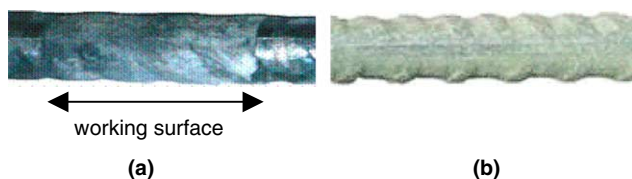


Fig. 8. Samples after 30 days of immersion in  $\text{Ca}(\text{OH})_2$  saturated solution: (a) GS, (b) CeGS.

Surface analysis with SEM coupled with EDS of GS and CeGS immersed in  $\text{Ca}(\text{OH})_2$  saturated solution for 30 days confirms changes in the composition and morphology of the surface. Fig. 9 shows the surface of the GS covered by a layer containing calcium and zinc. This passive layer is well known and described in literature [1,9,13–18]. As it was mentioned before, there is an initial dissolution of zinc as zincate ions  $\text{Zn}(\text{OH})_4^{2-}$  accompanied with hydrogen release for fresh concrete or  $\text{Ca}(\text{OH})_2$  saturated solutions at pH value of 13.3 or lower. Then, the surface is passivated by a layer of calcium hydroxyzincate  $\text{Ca}[\text{Zn}(\text{OH})_3]_2 \cdot 2\text{H}_2\text{O}$ .

CeGS specimens exhibit morphological changes with respect to the initial cerium conversion coating appearance (Fig. 10) together with high calcium concentration revealed in EDS analyses. The small white grains on the surface seem to be mainly composed of zinc oxides according to EDS analyses. After 30 days of immersion in  $\text{Ca}(\text{OH})_2$  saturated solution, as CeGS is rinsed and brushed, cerium is detected in the EDS analysis (Fig. 11) which indicates that

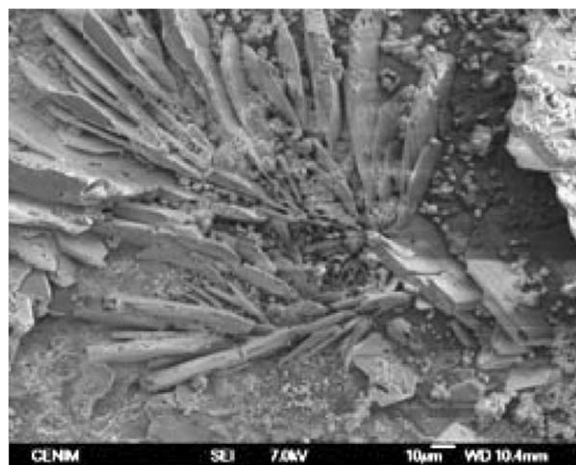


Fig. 9. SEM micrograph of GS surface after 30 days of immersion in  $\text{Ca}(\text{OH})_2$  saturated solution.

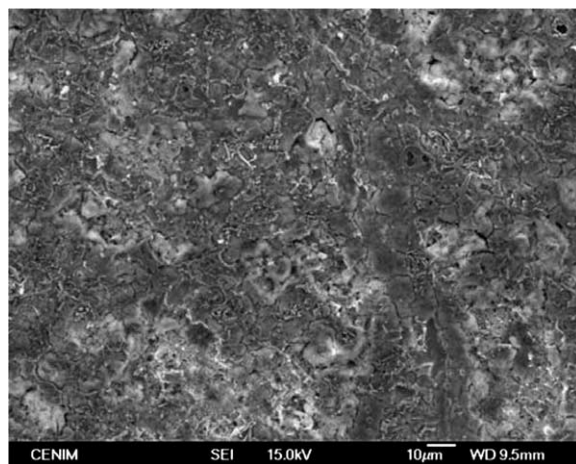


Fig. 10. SEM micrograph of CeGS initial surface before immersion in  $\text{Ca}(\text{OH})_2$  saturated solution.

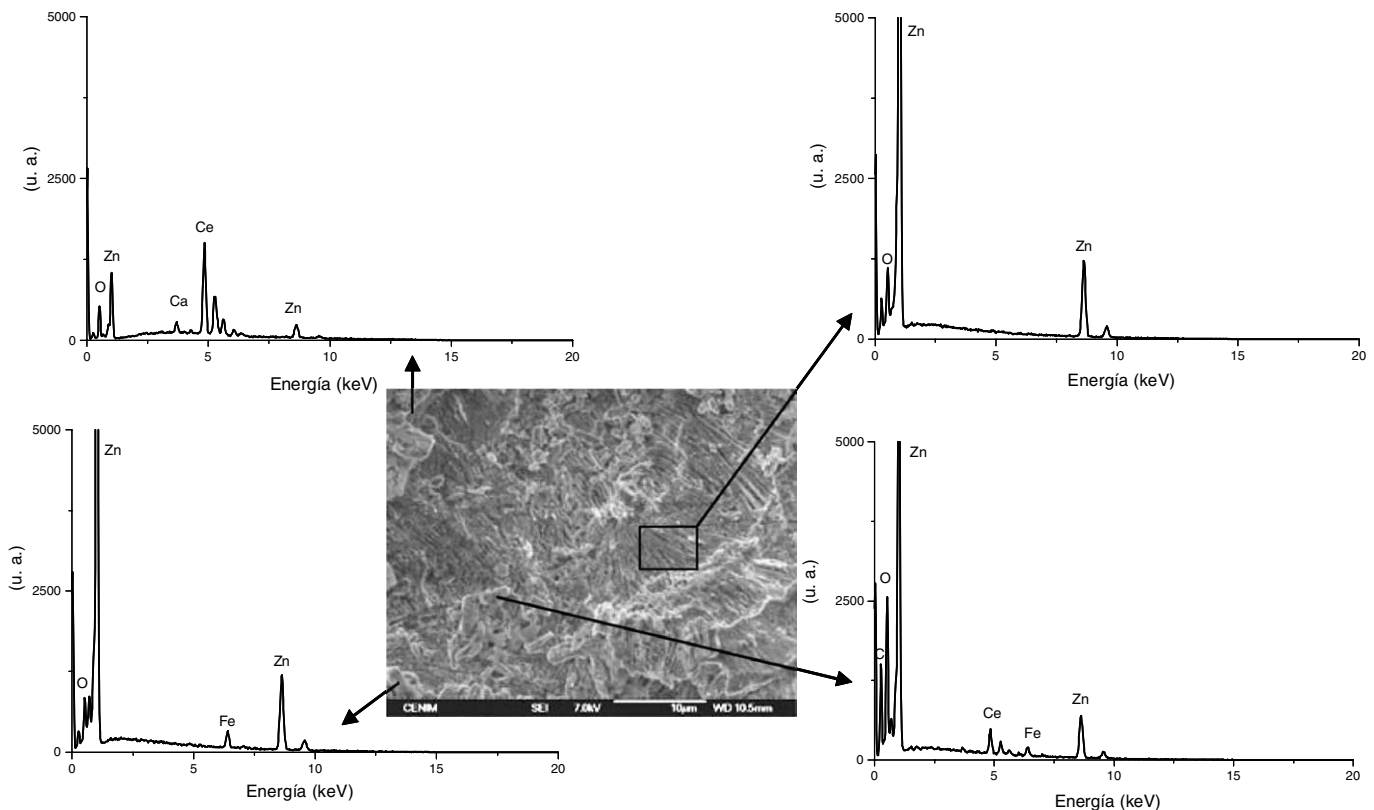


Fig. 11. Surface analyse by SEM coupled with EDS of CeGS after 30 days of immersion in  $\text{Ca}(\text{OH})_2$  saturated solution, rinsed with distilled water and brushed.

the cerium still remains in several areas of the surface after immersion in the alkaline solution. However, the results suggest that the presence of cerium on the surface does not provide good corrosion performance (see Fig. 7). This fact could be related to the cerium layer attack by the chloride ions which leaves the zinc surface exposed to the aggressive electrolyte.

X-ray diffraction analyses of CeGS and GS corrosion products formed after 50 days of immersion in  $\text{Ca}(\text{OH})_2$  saturated solution containing chlorides, indicate that simi-

lar compounds are formed on both specimens (Fig. 12): simonkolleite  $\text{Zn}_5(\text{OH})_8\text{Cl}_2 \cdot \text{H}_2\text{O}$  (JCPDS Cards 7-155), zincite  $\text{ZnO}$  (JCPDS Cards 36-1451), hydrozincite  $\text{Zn}_5(\text{CO}_3)_2(\text{OH})_6$  (JCPDS Cards 19-1458), and an hydrated shape of hydrozincite  $\text{Zn}_4\text{CO}_3(\text{OH})_6 \cdot \text{H}_2\text{O}$  (JCPDS Cards 11-0287). Calcite  $\text{CaCO}_3$  (JCPDS Cards 5-586) and sodium chloride  $\text{NaCl}$  (JCPDS Cards 5-628) were also found. Therefore, no cerium compounds have been identified, confirming the electrochemical results where cerium conversion coating does not provide an extra resistance with time to chlorides attack and pH condition at longer exposure time. In this case, precipitates from the test solution of CeGS were also analysed by XRD. Calcite and sodium chloride were only found revealing that cerium concentration is too small to be detected by XRD analyses.

Corrosion products indicated by XRD analyses are currently reported in literature for atmospheric corrosion of zinc and galvanized steel and for galvanized reinforcements when concrete is degraded by chlorides. Indeed,  $\text{Zn}_5(\text{OH})_8\text{Cl}_2 \cdot \text{H}_2\text{O}$  is found in chloride contaminated concrete [7,15,19] and is considered as a dangerous product responsible of the cracking of the concrete cover. It is also identified for zinc [20] and galvanized steel, used or not as construction material [21], exposed to atmospheric corrosion in presence of chlorides.  $\text{ZnO}$  is as well identified in atmospheric exposure [21] and in case of corrosion of galvanized reinforcements in alkaline solutions [15], concrete

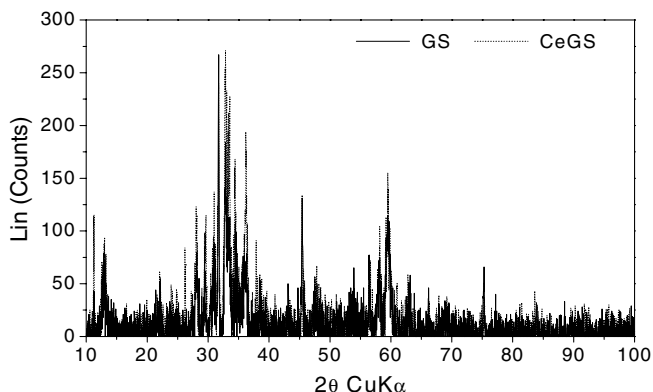


Fig. 12. X-ray diffractograms of corrosion products formed on CeGS and GS surface after 50 days in  $\text{Ca}(\text{OH})_2$  saturated solution  $+0.5 \text{ M Cl}^-$ .

structure [19,22] or concrete specimens [9].  $\text{Zn}_5(\text{CO}_3)_2(\text{OH})_6$  is reported in literature as a corrosion product of zinc in atmospheric conditions [21] and it has been found in concrete structure damaged by chlorides [19]. Its hydrated compound  $\text{Zn}_4\text{CO}_3(\text{OH})_6 \cdot \text{H}_2\text{O}$  and crystallized NaCl [20,21] are only described for atmospheric corrosion of zinc or galvanized steel in marine environment. Several authors assumed that NaCl crystallisation on surface points is a precursor of simonkolleite formation ( $\text{Zn}_5(\text{OH})_8\text{Cl}_2 \cdot \text{H}_2\text{O}$ ). Presence of calcite, hydrozincite and its hydrated compound are due to carbonation with time of  $\text{Ca}(\text{OH})_2$  saturated solution.

#### 4. Conclusion

New protective coatings have been developed by cerium conversion coating on galvanized reinforcements to prevent corrosion in concrete.

Cerium conversion coatings are composed of a mixture of cerium ( $\text{Ce}^{3+}$  and  $\text{Ce}^{4+}$ ) hydrated oxides/hydroxides with zinc oxide, ZnO, which thickness varies from 0.8 to 5  $\mu\text{m}$  because of the particular steel geometry due to the corrugations on the rebars.

In  $\text{Ca}(\text{OH})_2$  saturated solution, it is observed that galvanized steel with cerium conversion coating is more resistant than galvanized steel up to 5 days. During first immersion days, zinc dissolves in the alkaline to give a complex hydroxyzincate that are followed by the precipitation of a layer of calcium hydroxyzincate,  $\text{Ca}[\text{Zn}(\text{OH})_3]_2 \cdot 2\text{H}_2\text{O}$ , whereas cerium coating seems to remain stable and protective. This would explain the different corrosion behaviour observed at this immersion time. The results suggest that the presence of cerium layer can inhibit the initial hydrogen evolution on the galvanized surface. From 10 to 30 days of immersion, galvanized steel covered by a passive layer of calcium hydroxyzincate seems to offer the same protective efficiency than galvanized steel with cerium conversion coating. The anodic dissolution of zinc could be inhibited by cerium presence on the surface avoiding the calcium hydroxyzincate formation on the whole surface. The formation of the passive layer could be only expected on the defective areas of the conversion coating.

In presence of chlorides, cerium conversion coating reveals better localized corrosion resistance than GS after short immersion times based on electrochemical test.

As exposure time increases, 2 days, similar corrosion behaviour has been observed for CeGS and GS. Indeed, the same corrosion products of zinc are found after 50 immersion days: zinc hydroxychloride (simonkolleite), zincite, zinc hydroxycarbonate (hydrozincite) and a hydrated compound of the last one. Calcite and sodium chloride are also detected in corrosion products and precipitates.

Therefore, cerium conversion coatings improve the corrosion resistance of galvanized steel in alkaline media, in absence or chlorides containing solutions, at short immersion times. At longer exposure times both materials exhibit

similar corrosion behaviour whether chlorides are present in the medium or not.

#### Acknowledgements

The authors gratefully acknowledge the European Federation of Corrosion (EFC) and the financial support of the national project MAT99-0625-C02-02 which enabled this work to be carried out.

#### References

- [1] Yeomans SR. Corrosion of the zinc alloy coating in galvanized reinforced concrete. In: NACE Corrosion/98. Paper No. 653. Houston, Texas, 1998.
- [2] Hinton BRW, Wilson L. The corrosion inhibition of zinc with cerous chlorides. *Corros Sci* 1989;29(8):967–75.
- [3] Aramaki K. Treatment of zinc surface with cerium(III) nitrate to prevent zinc corrosion in aerated 0.5 M NaCl. *Corros Sci* 2001;43(11):2201–15.
- [4] Montemor M, Simões AM, Ferreira MGS. Composition and corrosion behaviour of galvanized steel treated with rare-earth salts: the effect of the cation. *Prog Org Coat* 2002;44(2):111–20.
- [5] Arenas MA, Damborenea JJ. XPS characterisation of cerium conversion layers on galvanized steel. In: Proc of 15th international corrosion congress, 2002.
- [6] Zhitomirsky I, Petric A. Electrochemical deposition of ceria and doped ceria films. *Ceram Int* 2001;27(2):149–55.
- [7] Bautista A, Gonzalez JA. Analysis of the protective efficiency of galvanizing against corrosion of reinforcements embedded in chloride contaminated concrete. *Cem Concr Res* 1996;26(2):215–24.
- [8] Yeomans SR. Performance of black, galvanized, and epoxy-coated reinforcing steels in chloride-contaminated concrete. *Corrosion* 1994;50(1):72–81.
- [9] Belaid F, Arliguie G, Francois R. Corrosion products of galvanized rebars embedded in chloride-contaminated concrete. *Corrosion* 2000;56(September):960–5.
- [10] Short NR, Zhou S, Dennis JK. Electrochemical studies on the corrosion of a range of zinc alloy coated steel in alkaline solutions. *Surf Coat Technol* 1996;79:218–24.
- [11] Dickson CL, Glasser FP. Cerium(III, IV) in cement implications for actinide(III, IV) immobilisation. *Cem Concr Res* 2000;30:1619–23.
- [12] Sherir LL, Jarman RA, Burstein GT. Corrosion, vol. 1. Great Britain: Butterworth Heinemann; 1994.
- [13] Macias A, Andrade C. The behaviour of galvanized steel in chloride-containing alkaline-solutions. I: The influence of the cation. *Corros Sci* 1990;30(4–5):393–407.
- [14] Nürnberger U. Supplementary corrosion protection of reinforcing steel. *Otto-Graf J* 2000;11:77–108.
- [15] Blanco MT, Andrade C, Macias A. SEM study of corrosion products of galvanized reinforcement immersed in solution in the pH range of 12.6–13.6. *Brit Corros J* 1984;19(1):41–8.
- [16] Belaid F, Arliguie G, Francois R. Porous structure of ITZ around galvanized and ordinary steel reinforcements. *Cem Concr Res* 2001;31(11):1561–6.
- [17] Fratesi R, Moriconi G, Coppola L. The influence of steel galvanization on rebars behaviour in concrete. In: Page CL, Barnforth P, Figg JW, editors. Corrosion of reinforcement in concrete construction. London: Cambridge, Royal Society of Chemistry; 1996.
- [18] Cheng A, Huang R, Wu JK, Chen CH. Effect of rebar coating on corrosion resistance and bond strength of reinforced concrete. *Constr Build Mater* 2005;19(5):404–12.
- [19] Bullard SJ, Covino BS, Holcomb GR, Cramer SD, McGill GE. Bond strength of thermally-sprayed zinc on concrete during early electrochemical aging. In: NACE Corrosion/97. Paper No. 232. New Orleans, March 10–14, 1997.



- [20] Neufeld A, Cole IS, Bond AM, Furman SA. The initiation mechanism of corrosion of zinc by sodium chloride particle deposition. *Corros Sci* 2002;44(3):555–72.
- [21] Seré P, Zapponi M, Elsner CI, Disarti AR. Comparative corrosion behaviour of 55 aluminium–zinc alloy and zinc hot-dip coatings deposited on low carbon steel substrates. *Corros Sci* 1998;40(10):1711–23.
- [22] Hime WG, Machin M. Performance variances of galvanized steel in mortar and concrete. *Corrosion* 1993;49(October): 858–60.